49th AIAA Aerospace Sciences Meeting including the New Horizons Forum and Aerospace Exposition
4 - 7 January 2011, Orlando, Florida

AIAA 2011-420

Performance Modeling of a Paraffin Wax / Nitrous Oxide Hybrid Rocket Motor

Bernard Geneviève[1], Michael J. Brooks[2], Jean-François P. Pitot de la Beaujardiere[3], and Lance W. Roberts[4]
School of Mechanical Engineering, University of KwaZulu-Natal, Durban, 4041, South Africa

This paper describes the development of a one-dimensional, non-steady flow predictive performance model for hybrid rocket motors. The analysis relies on basic thermodynamic and gas dynamic assumptions. The analytical model was programmed in MATLAB and uses the NASA-CEA equilibrium chemistry code to determine gas combustion properties. An empirical regression rate correlation is employed in the model with ballistic coefficients found in the literature. The predictive model implements conservation of mass and the ideal gas equation of state to compute changes in chamber pressure. Instantaneous performance parameters such as theoretical thrust and specific impulse can be analyzed for different operating conditions defined by the user. To validate the analytical model, a laboratory-scale motor has been designed and manufactured using a paraffin wax and nitrous oxide propellant combination. Hot-fire test data are compared with the predictive modeling.

Nomenclature

A	=	cross-sectional area, m^2
a	=	ballistic regression rate coefficient
C_d	=	injector discharge coefficient
C_F	=	thrust coefficient
c^*	=	characteristic velocity, m/s
D_f	=	final port diameter, m
D_i	=	initial port diameter, m
d	=	diameter, m
F	=	thrust, N
G	=	total mass flux, kg/m^2s
g	=	gravitational acceleration, m/s^2
He_v	=	helium vapor
Isp	=	specific impulse, s
L_g	=	fuel grain length, m
M_{He}	=	loaded helium mass, kg
M_{N_2O}	=	loaded nitrous oxide mass, kg
M_t	=	oxidizer tank mass, kg
m	=	ballistic regression rate coefficient
m_c	=	gaseous mass stored in chamber, kg
$\dot{m}$	=	mass flow rate, kg/s
MW	=	molecular weight, kg/kmol
N_{inj}	=	number of injectors
$(N_2O)_l$	=	liquid nitrous oxide
$(N_2O)_v$	=	vapor nitrous oxide
n	=	ballistic regression rate coefficient
O/F	=	oxidizer-to-fuel ratio
P	=	pressure, Pa
P_{c_o}	=	initial chamber pressure, Pa
P_{losses}	=	feed system pressure drop, Pa
P_t	=	oxidizer tank pressure, Pa
R_c	=	combusted specific gas constant, $J/kg.K$
R_p	=	instantaneous port radius, m
$\dot{r}$	=	regression rate, m/s
T	=	temperature, K
T_t	=	oxidizer temperature in tank, K
v	=	gas velocity, m/s
v_{exh}	=	effective exhaust gas velocity, m/s
V_c	=	chamber volume, m^3
V_t	=	oxidizer tank volume, m^3
x	=	port length coordinate, m
α	=	divergence cone angle, deg
η_c	=	combustion efficiency
λ	=	divergence cone loss

[1] Graduate student, School of Mechanical Engineering, Durban, 4041. AIAA Student Member.
[2] Senior Lecturer, School of Mechanical Engineering, Durban, 4041. AIAA Member.
[3] Lecturer, School of Mechanical Engineering, Durban, 4041. AIAA Member.
[4] Professor, School of Mechanical Engineering, Durban, 4041. Non-member of AIAA.

ρ	=	density, kg/m^3

Subscripts

a	=	atmospheric property
c	=	chamber
cor	=	corrected
f	=	fuel
inj	=	injector
model	=	model analysis
noz	=	nozzle flow analysis
ox	=	oxidizer flow analysis
the	=	theoretical analysis
t	=	nozzle throat condition
2	=	nozzle outlet condition

I. Introduction

Conventional hybrid rocket motors produce thrust by chemically combusting a liquid or gaseous oxidizer with a solid fuel grain in a combustion chamber. The fuel grain erodes and vaporizes as the oxidizer is injected into the high-pressurized chamber vessel. Hybrid propulsion systems offer attractive characteristics compared to solid and liquid rocket motors, including a high degree of operational safety, design simplicity, full thrust control and overall cost effectiveness.

This paper discusses and models the performance of a laboratory-scale paraffin wax and nitrous oxide propulsion system. Paraffin fuel is selected due to its high regression rate. Previous experiments[1] have shown that the regression rate of paraffin-based fuel is three to four times higher than classical hybrid fuels. Liquid nitrous oxide as oxidizer offers inherent advantages such as it is relatively cheap and available, non-toxic, self-pressurizing, and subcritical (storable) at room temperature. A disadvantage is that the optimum oxidizer-to-fuel ratio is higher compare to other standard oxidizers, hence, the design results in a heavier flight motor system. Nitrous oxide decomposes into nitrogen and oxygen at a temperature of 520°C [2]. Upon decomposition, the inert nitrogen facilitates erosion of the fuel grain and helps to cool the motor nozzle. Melted paraffin combusts with the oxygen forming the superheated thermodynamic gas products.

A Hybrid Rocket Performance Code (HRPC) was developed to predict motor performance under different operating specifications and conditions. The code functionality is not restricted to liquid nitrous oxide and paraffin-wax analysis, but can also aid in characterizing the combustion of various classical propellant combinations. A laboratory-scale motor[3] and test stand[4] were designed, fabricated, and tested to validate the analytical model. Suggestions are made to address and improve the current limitations of the modeling. Investigation and analysis of a series of lab-scale motor tests is currently being conducted to assist in the development process of a hybrid flight motor. This larger motor is intended for use in the first phase of the Hybrid Sounding Rocket Program being developed at the University of KwaZulu-Natal[5]. The flight motor will be tested prior to launch to validate its predicted performance and then used in UKZN's Phoenix-1A 10 km apogee test vehicle being developed in a parallel project[6]. As part of that work a six degree-of-freedom trajectory simulation software is developed for small hybrid sounding rockets. We aim to integrate the hybrid rocket predictive performance model with the trajectory simulation for optimization of the 10 km sounding rocket.

II. Analytical Modeling

In this study, the performance model of the hybrid rocket motor consists of three coupled parts, depicted as control volumes one to three in Fig 1. Basic thermodynamic and gas dynamic assumptions govern the analysis of the modeling, including ideal gas theory. Firstly, the oxidizer mass flow rate is characterized by the discharging process of the tank in CV1. Blowdown of the oxidizer tank is driven by a combination of nitrous oxide self-pressurization and helium gas supercharging, in addition to the pressure difference between the tank and the combustion chamber. Secondly, the modeling of the combustion within CV2 is analyzed through the regression rate of the fuel grain and the change in the thermochemistry of both propellants. The performance of the rocket motor is significantly influenced by the increase in chamber pressure resulting from the buildup of combusted gases flowing through the constricted nozzle throat. Thirdly, the rocket nozzle function is to accelerate the gas flow to supersonic velocity at the nozzle outlet thereby producing the thrust. The mass flow rate of the combustion products within CV3 is the driving input in determining the flow velocity at the nozzle outlet.

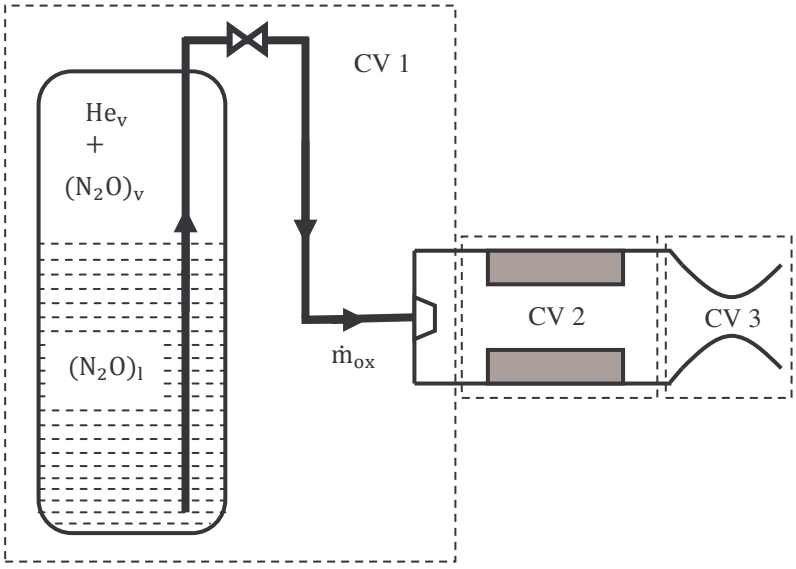

Figure 1. Three distinct control volumes are modeled.

A. Oxidizer Tank Pressurization and Discharging

Analysis of hybrid motor performance begins with the modeling of the fluid properties within CV1. The working fluids are single-phase helium vapor and two-phase nitrous oxide liquid-vapor mixtures. Being sub-critical at room temperature in the closed tank, nitrous oxide is a self-pressurizing fluid. Helium vapor assists the blowdown of liquid nitrous oxide by pressurizing the oxidizer tank above the vapor pressure of nitrous oxide. Properties of the pressurizing system change as the tank empties with time. Modeling this change in the fluid thermodynamic state is critical for determining the oxidizer mass flow rate through the injector and in the combustion chamber. The thermodynamic state variation of nitrous oxide is significantly dependent on the environmental oxidizer tank temperature and on the liquid nitrous oxide mass flow out of CV1. A change in thermal energy of the tank walls disturbs the liquid-vapor equilibrium balance mixture. As well as, a change in thermal energy of liquid nitrous oxide as the tank drains out causes a shift in the ratio of liquid to vapor mass.

By evaluating the nitrous oxide vapor temperature and liquid-vapor mass within the tank, the vapor pressure can be modeled. The mathematical modeling from ref. (7) is used for the analysis of the tank pressurization and discharging. The model assumes Ideal Gas Law and Raoult's Law. The oxidizer mass flow rate through the injector is determined from:

$$\dot{m}_{ox} = C_d A_{inj} N_{inj} \sqrt{2\rho_{ox}(P_t - P_{losses} - P_c)} \tag{1}$$

where C_d is the dimensionless discharge coefficient, A_{inj} the cross-sectional area of the orifice, N_{inj} the number of orifices, ρ_{ox} the oxidizer density, P_t the tank pressure, P_{losses} the pressure drop in the feed system and through the injector, and P_c the chamber pressure.

B. Fuel Regression Rate

The prediction of fuel regression rate is limited to the empirical correlation from classical hybrid theory developed by Marxman et al[8]:

$$\dot{r} = aG^n x^m \tag{2}$$

where a, n, and m are the ballistic coefficients, and x is the distance down the port. This states that regression rate is dependent on both total mass flux and port length coordinate. The three ballistic coefficients are determined experimentally for a specific oxidizer and fuel combination. From literature, the exponent m tends to be much less

than one, so in this study the space variation is ignored ($m = 0$). The regression rate empirical formula[9] can be simplified as:

$$\dot{r} = aG_{ox}^{n} \tag{3}$$

where G_{ox} is the oxidizer mass flux, which is equal to the instantaneous oxidizer mass flow rate over grain port cross-sectional area. The time-marching equations are depicted in Fig. 4.

C. Combustion Chamber Gas Analysis

Characterizing the combustion chemistry of a rocket motor is crucial. It determines the manner in which oxidizer and fuel react to form useful thermodynamic gases at a particular flame temperature. Once the propellants are ignited, the combustion process is self-sustained until one or both propellant components are depleted. The combustion efficiency, η_c, is a function of the oxidizer-to-fuel ratio effectiveness, and chamber pressure. The latter depends on the change in gaseous products stored in the chamber, gaseous mass flow through the nozzle, and nozzle throat cross-sectional area. Hybrid rocket motors that employ feed systems without high pressure pumps, notice a decrease in oxidizer flow rate with time. This decrease contributes to the change in combustion efficiency and thus rocket performance. As a result, a non-steady state analysis of the combustion process needs to be modeled.

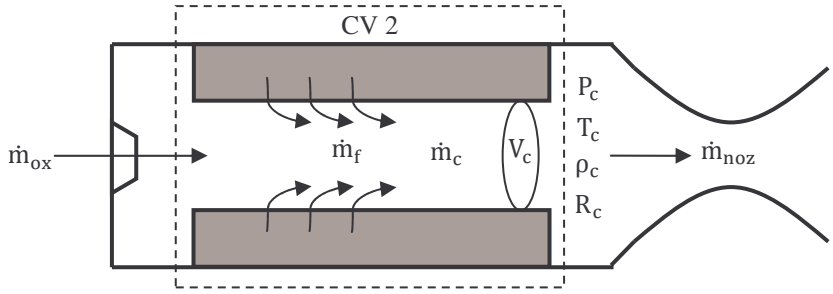

Figure 2. Combustion chamber control volume 2.

Control volume, CV2, is assigned around the combustion chamber (Fig. 2) and the following assumptions are implemented to simplify the mathematical model: (1) the combustion products behave as a perfect gas, (2) the propellant mass stored within CV2 is non-uniform due to the change in chamber volume and gaseous mass flow out of the nozzle, (3) pre- and post- combustion volumes are assumed negligible, (4) change in spatial thermodynamic gas properties are deemed negligible due to the size of the lab-scale motor, (5) uniform regression rate is assumed across the fuel grain, and (6) no heat transfer through the chamber wall.

The analytical model is derived from first principles. Using the conservation of mass to determine the change of gaseous mass in CV2, the mass stored in the chamber is defined as:

$$\dot{m}_c = \dot{m}_{ox} + \dot{m}_f - \dot{m}_{noz} \tag{4}$$

where the mass generated from the combustion process is given by the total of oxidizer and fuel mass flow rates, $\dot{m}_t = \dot{m}_{ox} + \dot{m}_f$. From ideal gas theory, the chamber pressure is a function of combustion properties: gaseous mass, volume, temperature, and density.

$$P_c = \frac{m_c R_c T_c}{V_c} \tag{5}$$

The non-steady state chamber pressure can be solved by differentiating Eq. (5) with respect to time. Modeling all properties as variable with time, the change in chamber pressure is determined by:

$$\frac{dP_c}{dt} = \frac{m_c}{V_c}\left[R_c\frac{dT_c}{dt} + T_c\frac{dR_c}{dt}\right] - \frac{R_c T_c}{V_c^2}\left[m_c\frac{dV_c}{dt} - V_c\frac{dm_c}{dt}\right] \tag{6}$$

D. Nozzle Gas Flow Analysis

In this study, we have modeled hybrid rocket motor performance using one-dimensional, non-steady gas flow theory across CV3. Basic gas flow assumptions form the base of the analysis (Fig. 3): (1) chamber, stagnation, and nozzle inlet gas properties are equivalent assuming negligible gas flow velocity at nozzle inlet, (2) isentropic nozzle expansion, (3) adiabatic combustion, (4) no shock waves in the nozzle flow, and (5) combustion products obey the ideal gas law.

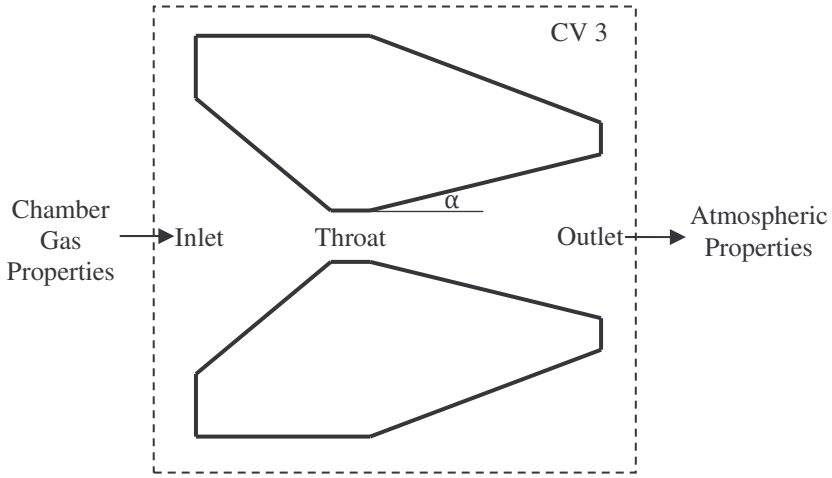

Figure 3. Nozzle gas flow modeling.

From the above assumptions, a series of fundamental equations[10] are applied to characterize performance. Two performance correction factors account for combustion efficiency of the gaseous species and for the divergence cone angle loss of the De-Laval nozzle.

$$c^*_{model} = \eta_c c^*_{the} \tag{7}$$

$$\lambda = \frac{1}{2}(1 + \cos\alpha) \tag{8}$$

To reach the supersonic flow condition in the diverging section of the nozzle, the flow must be choked at the throat. The nozzle mass flow rate determined from the standard choked flow equation is a function of chamber pressure, nozzle throat cross-sectional area, and thermodynamic gas properties (implicit in the characteristic velocity) which define sonic condition at the throat.

$$\dot{m}_{noz} = \frac{P_c A_t}{c^*_{model}} \tag{9}$$

The divergence angle correction factor, λ, alters the theoretical motor performance by correcting the nozzle exit velocity component only in the thrust coefficient, C_F, exhaust velocity, V_{exh}, and thrust, F, formulae. Specific impulse, Isp, gives a fundamental measure of performance, by which comparison with other motors is possible. It is defined as the thrust per unit weight of propellant.

$$C_F = \frac{\lambda v_2}{c^*_{model}} + \left(\frac{P_2 - P_a}{P_c}\right)\frac{A_2}{A_t} \tag{10}$$

$$v_{exh} = c^*_{model} C_F \tag{11}$$

$$F = \dot{m}_{noz} v_{exh} \tag{12}$$

$$Isp = \frac{\lambda v_2}{g} + \frac{(P_2 - P_a)A_2}{\dot{m}_{noz} g} \tag{13}$$

III. Hybrid Rocket Performance Code

From the theory described above, a software tool was developed to predict performance of hybrid motors and to assist in overall design optimization. The Hybrid Rocket Performance Code (HRPC) is programmed in MATLAB and interacts with NASA's Chemical Equilibrium with Applications (CEA) program[11] to model non-steady state combustion in the motor chamber. The use of NASA-CEA permits solution of Equations (5) to (13) in the HRPC application, which calls combustion parameters automatically during execution. This interaction is achieved by creating an input file with the problem fully stated, running NASA-CEA, and reading calculated data from the output file at each time step. Consequently, the gas properties are solved incrementally which enables the instantaneous analysis of the rocket motor performance.

Key features of the HRPC program (Fig. 4) are: (1) user defined parameters, (2) an option to select between modeling of the oxidizer tank blowdown or constant oxidizer mass flow, and (3) an option to define the appropriate NASA-CEA input subroutines for a specific rocket motor analysis. The user has the option to run HRPC with constant oxidizer mass flow if a pressurization feed pump system is utilized in the design. Different input subroutines can be defined in NASA-CEA through the MATLAB code, including frozen or equilibrium flow analysis.

If the oxidizer tank blowdown is being modeled, HRPC determines the initial conditions within the tank and combustion chamber prior to running. As it executes, the oxidizer mass flow rate is calculated from Eq. (1), where the initial chamber pressure is equal to the atmospheric pressure. The liquid oxidizer mass flow out of the tank results in changes to tank temperature and pressure. Volumetric chamber expansion is characterized by the pyrolyzing of the fuel grain port. The user defined combustion efficiency, η_c, is scaled to match the experimental data. Typical combustion efficiencies for hybrid rocket motors range from 85% to 95% [10]. The oxidizer-to-fuel ratio resulting from the regression rate modeling and the chamber pressure is integrated into the input file to run NASA-CEA. Useful parameters such as characteristic velocity and thrust coefficient from NASA-CEA are passed to the MATLAB code, which in turn solves for the motor performance (Eq. (12) and (13)). Prior to the motor performance calculations, the thrust coefficient from NASA-CEA must be corrected for the appropriate atmospheric pressure since the software assumes that the calculated exit pressure is equal to the ambient pressure, which leads to inaccurate modeling of the gas flow. Similarly, the specific impulse must be modified to the working atmospheric pressure. The second terms on the right hand sides of Eq. (10) and (13) vanish in NASA-CEA, which instead uses Eq. (14) and (15), respectively.

$$C_F = \frac{v_2}{c^*} \tag{14}$$

$$Isp = \frac{v_2}{g} \tag{15}$$

Figure 5 illustrates a typical discrepancy in specific impulse analysis between HRPC and NASA-CEA. The following conditions were applied in the modeling; to simulate expected performance from a laboratory-scale hybrid rocket motor under development at UKZN:

a) Chamber pressure of 40 bar.
b) Sea level atmospheric pressure of 1.01325 bar.
c) Assumed constant nozzle gas mass flow of 0.35 kg/s.
d) Conical nozzle.
e) Paraffin wax and nitrous oxide propellant combination.
f) Propellants initial temperature of 25°C.
g) Shifting equilibrium gas analysis.

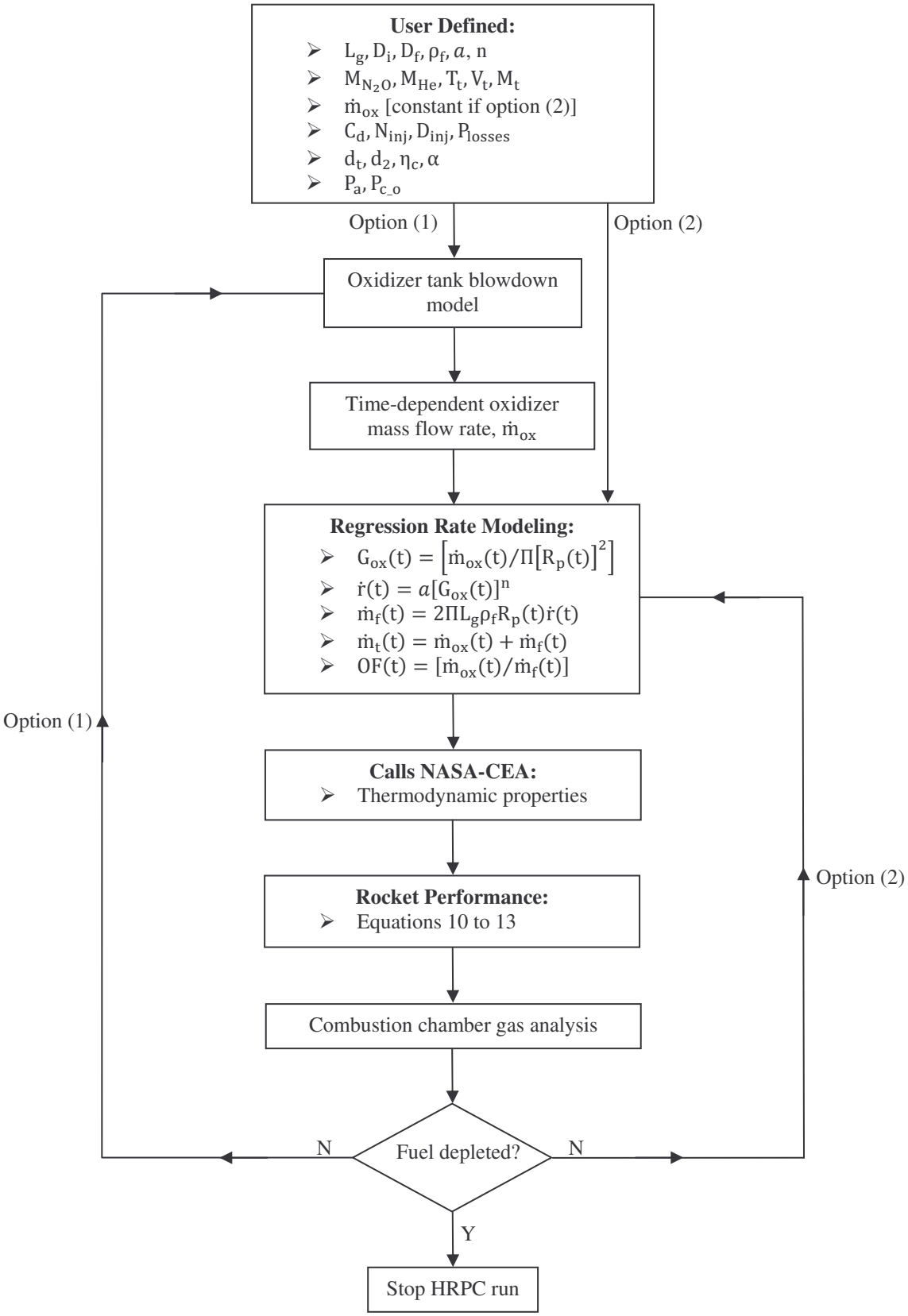

Figure 4. Hybrid Rocket Motor Performance Code.

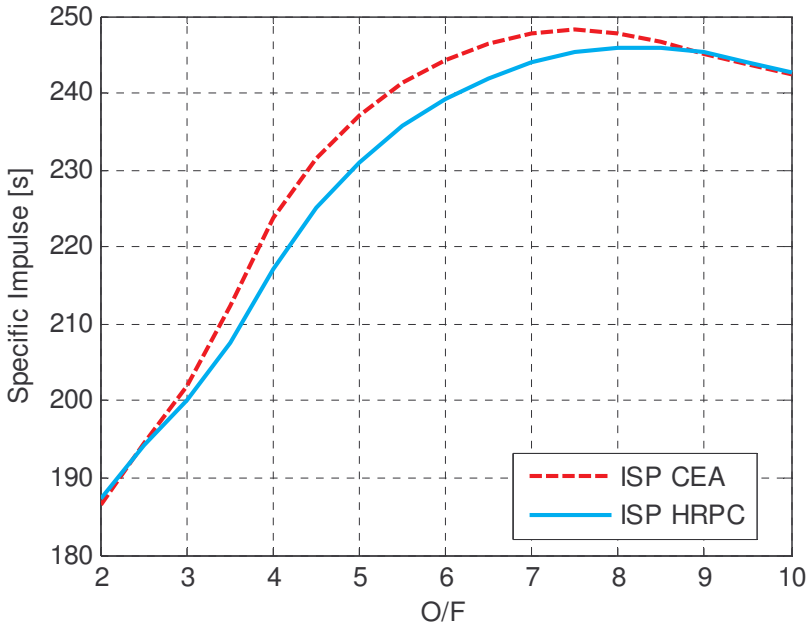

Figure 5. Specific impulse correction to NASA-CEA.

IV. UKZN PL-1 Laboratory Scale Motor

Design of the UKZN laboratory test facility was focused on reusability and flexibility to enable regular hybrid rocket motor testing. The modular design offers advantages in characterizing different oxidizer and fuel combinations to optimize a specific hybrid rocket propulsion system. The motor permits interchanging of the injector configurations, pre- and post- combustion chamber material inserts, fuel grain cartridges, and nozzles. The PL-1 lab-scale motor main body is manufactured from two 6061-T60 aluminum blocks and 316L grade stainless steel tubing. The blocks accommodate an adjustable injector head configuration and the nozzle is machined from graphite. High tensile steel bars hold the motor components in compression. The fuel grain cartridge is constrained by the combustion chamber dimensions. Fuel grain lengths and outer diameters up to 200 mm and 64 mm, respectively, can be tested with the current casing. A paraffin wax manufactured by SASOL (0907) was selected for use as the fuel, and a grain casting technique that minimizes shrinkage and porosity was developed at UKZN. The grain cartridge is rolled inside a thermal liner that insulates the motor from the hot combusted gas. The lab-scale motor specifications are given in Table 1. Ballistic coefficients ($\dot{r}$ in mm/s, G_{ox} in g/s-cm^2) are adopted from previous experimental data[12].

Table 1. Lab-scale motor design specifications.

Paraffin Wax[12]	Formula	$C_{50}H_{102}$
	Density, kg/m^3	924
	Enthalpy of formation, KJ/mole	-1438.2
Ballistic Coefficients[12]	a	0.472
	n	0.555
Grain length, m		0.160
Inner grain diameter, m		0.032
Outer grain diameter, m		0.064
Nozzle outlet diameter, m		0.0314

The oxidizer feed system consists of thermocouples, pressure transducers, valves and associated fittings. Oxidizer and purge systems are controlled by automatically actuated ball and solenoid valves. For safety, relief, bleed and check valves were included in the feed system design. Inert helium gas is used to maximize the nitrous oxide liquid-phase in the pipe and to prevent cavitation. Nitrogen purge gas is employed as the combustion chamber cooling agent. Remote and automatic operation of the overall system is achieved through National Instruments CompactRIO data acquisition and control system with a programmable LabVIEW interface. The LabVIEW code provides an automated run sequence and takes full control of the lab-scale motor tests. The instantaneous tank mass is monitored and relayed to the CompactRIO for data capturing. The test facility is shown in Fig. 6.

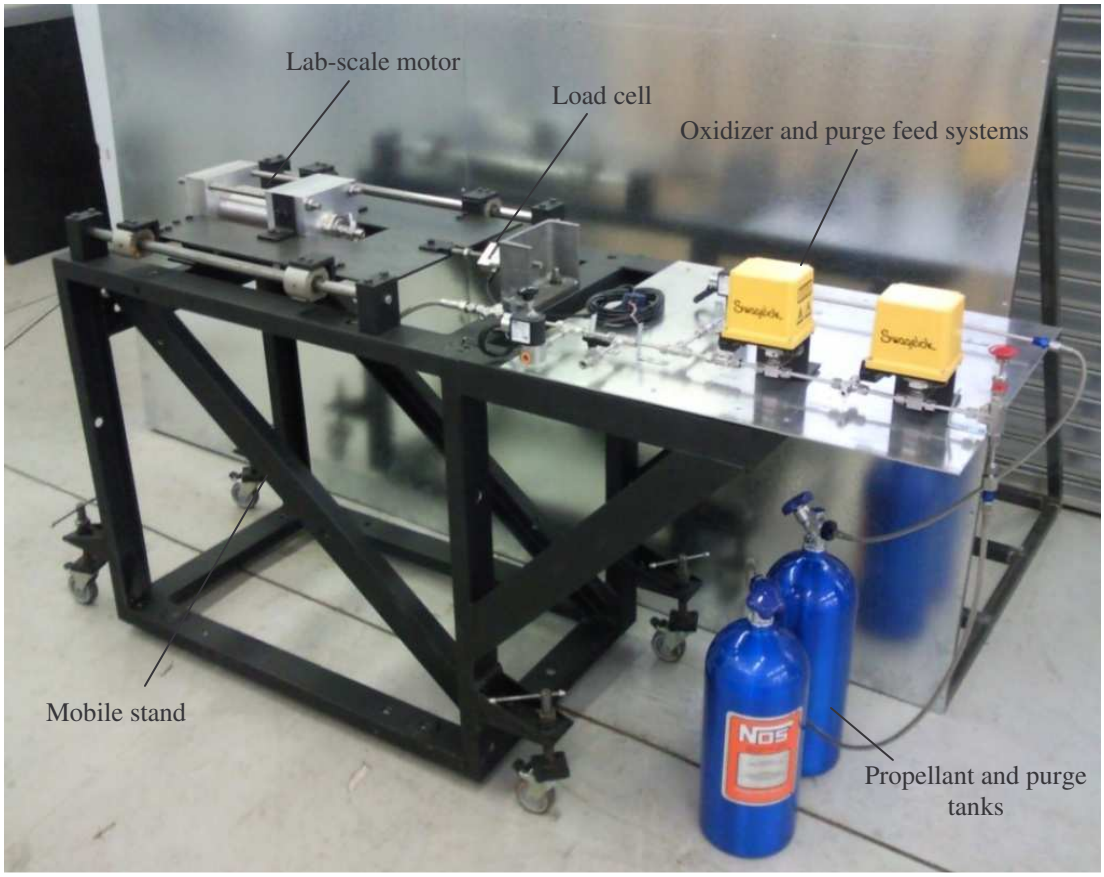

Figure 6. Assembled UKZN hybrid rocket motor test cell.

V. Numerical and Experimental Results

Hot-fire testing of the first PL-1 lab-scale hybrid rocket motor was started in October 2010. Two types of test generally need to be conducted: (1) cold-flow tests, and (2) hot-fire tests. A series of cold-flow tests was performed to characterize the initial oxidizer mass in the tank and flow rate needed for full burnout of the fuel grain. These tests were carried out with no grain cartridges. In addition, different igniter firing sequences were experimented to ensure successful ignition and self-sustained combustion of the propellants. A photograph of the motor plume during the first hot-fire test is shown in Fig. 7.

Figure 8 shows the experimental and theoretical thrust profiles for the first test. The automatically actuated flow control valve is opened and closed at 0 and 10 seconds, respectively. A peak thrust of 631 N is reached at igniter burnout, and full combustion was sustained for 6.5 sec until depletion of the paraffin-wax grain. A noticeable drop in thrust at fuel grain burnout was experienced and it is assumed that the burning of pre- and post- combustion chamber inserts contributed to this thrust with unchoked flow condition. The thrust spike prior to the tail-off phase is likely due to a buildup in chamber pressure as fuel grain fragments momentarily blocked the nozzle.

Figure 7. Inaugural laboratory-scale test of UKZN's PL-1 motor.

Two theoretical curves are depicted in Fig. 8. The predicted theoretical thrust profile was modeled for the ideal operating conditions of the lab-scale motor. During the motor test, both the chamber pressure and oxidizer flow rate were lower than the targeted design parameters, therefore to verify the analytical model, the average experimental oxidizer mass flow rate was implemented in the model to give modeled thrust curve, shown in Fig. 8. The model thrust data agree fairly well with the experimental results. Frozen nozzle gas flow analysis was assumed in the model together with a fixed injector discharged coefficient. The ignition burn process is modeled as a ramp function. The discrepancy between fuel burnout times is likely due to unburnt grain fragments being ejected from the motor at start-up. The model under-predicts chamber pressure and thrust performances towards the end of the run. Being coupled to the chamber pressure, the oxidizer-to-fuel ratio greatly affects the flame temperature and thrust performance and an underestimated O/F ratio can lower performance.

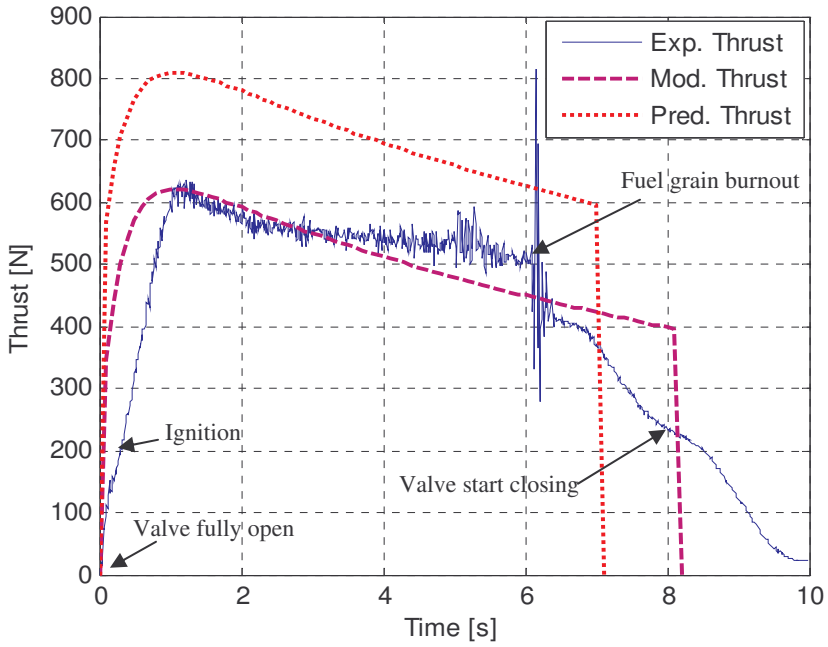

Figure 8. Time history of thrust profiles.

Data from the modeled thrust run were used to deduce key performance parameters of the hybrid rocket motor. Results are given in Fig. 9. The instantaneous regression rate, oxidizer-to-fuel ratio, and oxidizer mass flux weaken throughout the burn because oxidizer flow rate decreases and port radius increases. Oxidizer mass flow rate decays with tank pressure as head space vapor volume expands with time. The burning of the grain cartridge increases the port cross-section area that causes a shift in oxidizer-to-fuel ratio and regression rate. A higher regression rate is associated with an increased oxidizer mass flux. The ballistic regression rate coefficients from ref. (12) could not be confirmed due to full consumption of the fuel grain.

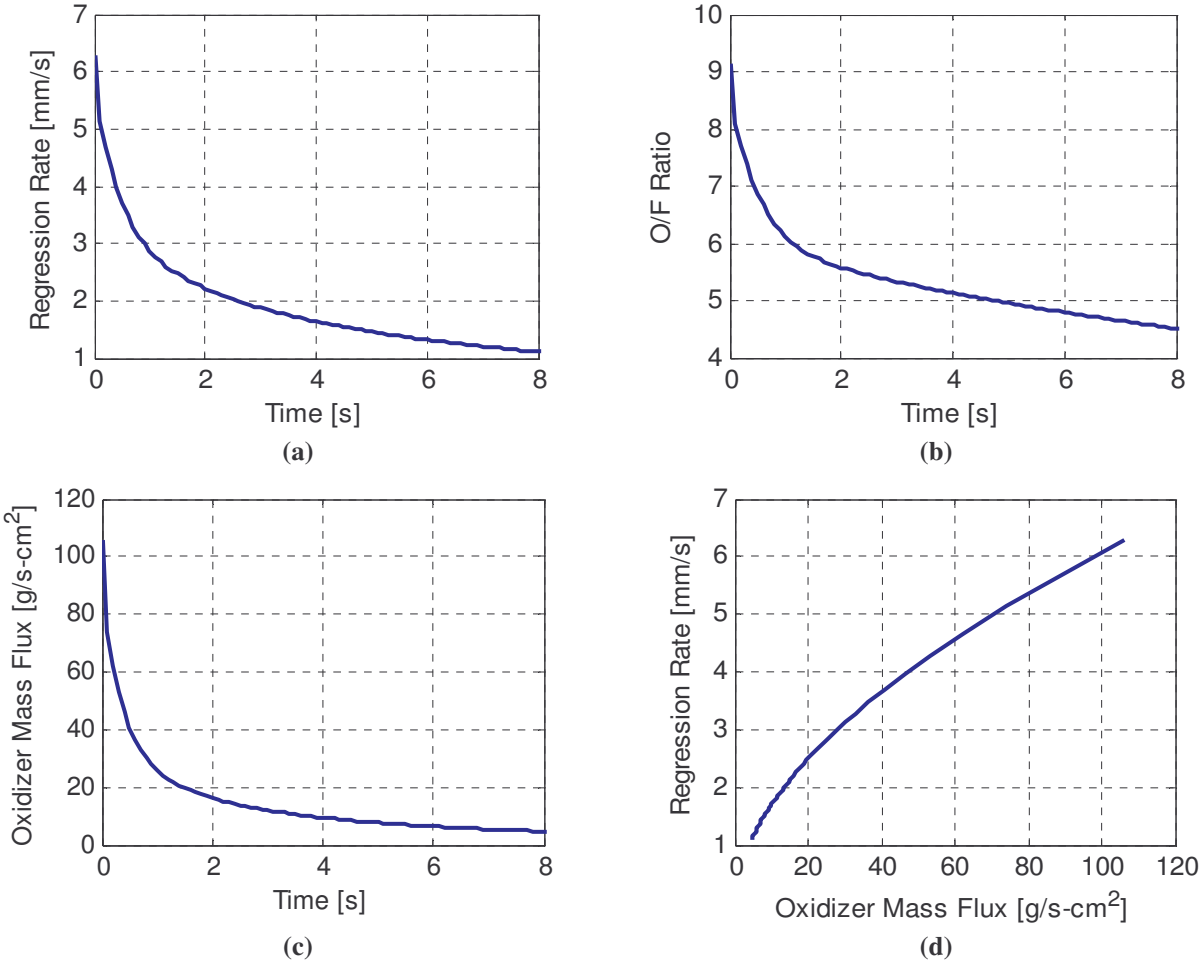

Figure 9. Modeled test run instantaneous performances.

VI. Conclusions

An analytical performance code has been developed for hybrid rocket propulsion systems using liquid nitrous oxide and paraffin-wax as the propellants. The code communicates with NASA-CEA equilibrium gas chemistry code to model changes in thermodynamic gas properties during combustion. In addition, it predicts the instantaneous rocket performance for different user defined operating conditions. Test data from a lab-scale hybrid rocket motor were compared with the predictive code, and show reasonable agreement. An inherent advantage of the code is that it can be used for different oxidizer and fuel combinations if the proper parameters are known. The current model has some limitations that will be addressed in the near future, one of which is the non-physical modeling of the regression rate. In addition, the modeling of the tail-off phase at the end of the run has not yet been completed. Further testing is planned to characterize the fuel regression rate correlation and overall performance of the UKZN PL-1 motor.

Acknowledgments

The authors thank Daniel Booyens, Sibusiso Mabaso, Bilal Goolam Mahomed, Serushin Moodley, Jivashan Reddy and Jonathan Smyth for their assistance in designing and manufacturing the lab-scale motor and test stand. The authors also wish to thank Mr. R. Bodger, SASOL and UKZN Innovation for guidance and support.

References

[1]Karabeyoglu, M. A., Altman, D., and Cantwell, B. J., "Combustion of Liquefying Hybrid Propellants: Part 1, General Theory," *Journal of Propulsion and Power*, Vol. 18, No. 3, May-June 2002.

[2]Zakirov, Z., Sweeting, M., Lawrence, T., Sellers, J., "Nitrous Oxide as a Rocket Propellant," *Acta Astronautica*, Vol. 48, No. 5-12, pp. 353-362, 2001.

[3]Booyens, D., Smyth, J., and Moodley, S., "Hybrid Rocket Motor Design," Undergraduate Final Year Report, School of Mechanical Engineering, University of KwaZulu-Natal, Durban, South Africa, 2010.

[4]Mabaso, S., Mahomed, B. G., and Reddy, J., "Hybrid Rocket Test Stand," Undergraduate Final Year Report, School of Mechanical Engineering, University of KwaZulu-Natal, Durban, South Africa, 2010.

[5]Brooks, M. J., Pitot de la Beaujardiere, J. F. P., Chowdhury, S. M., Geneviève, B., and Roberts, L. W., "Introduction to the University of KwaZulu-Natal Hybrid Sounding Rocket Program," *46th AIAA/ASME/SAE/ASEE Joint Propulsion Conference & Exhibit*, 25-28 July 2010, Nashville, TN.

[6]Chowdhury, S. M., Brooks, M. J., Pitot de la Beaujardiere, J. F. P., "Improved Design of Hybrid Rockets Using a 6 Degree-of-Freedom Trajectory Simulator," *49th AIAA Aerospace Sciences Meeting,* 4-7 Jan 2011, Orlando, Florida, Submitted.

[7]Fernandez, M. M., "Propellant Tank Pressurization Modeling for a Hybrid Rocket," Masters Thesis, Department of Mechanical Engineering, Rochester Institute of Technology, NY, 2009.

[8]Marxman, G. A., Wooldridge, C. E., and Muzzy, R. J., "Fundamentals of Hybrid Boundary Layer Combustion," *Progress in Aeronautics and Astronautics*, Vol. 15, 1964, pp. 485-522.

[9]Chiaverini, M. J., and Kuo, K. K., Fundamentals of Hybrid Rocket Combustion and Propulsion, AIAA, Progress in Astronautics and Aeronautics, Vol. 218.

[10]Sutton, G., and Biblarz, O., Rocket Propulsion Elements, 7th Edition, John-Wiley & Sons, New York, 2001.

[11]Gordon, S., and McBride, B. J., "Computer Program for Calculation of Complex Chemical Equilibrium Compositions and Applications," NASA RP-1311, 1994.

[12]Grosse, M., "Development Work on a Small Experimental Hybrid Rocket," *33rd AIAA/ASME/SAE/ASEE, Joint Propulsion Conference & Exhibit*, July 6-9, 1997, Seattle, WA.